University of BRISTOL

Going beyond SI searches with LUX-ZEPLIN

Sam Eriksen, on behalf of the LZ Collaboration

Lake Louise Winter Institute 2024

19th February 2024

The LUX-ZEPLIN Detector

Dual Phase Time Projection Chamber

- Primary scintillation light (S1)
- Secondary scintillation induced from free charge (S2)
- 3D reconstruction allows for fidualisation
- ER/NR discrimination from S1:S2 ratio

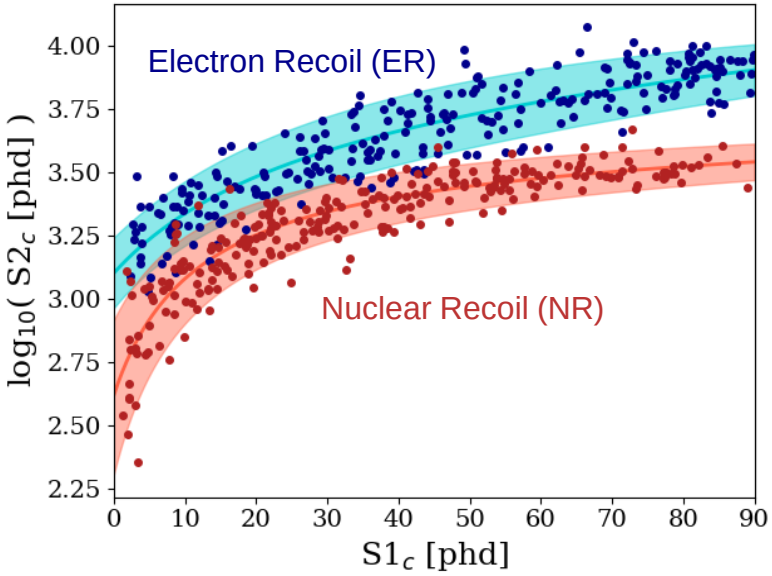

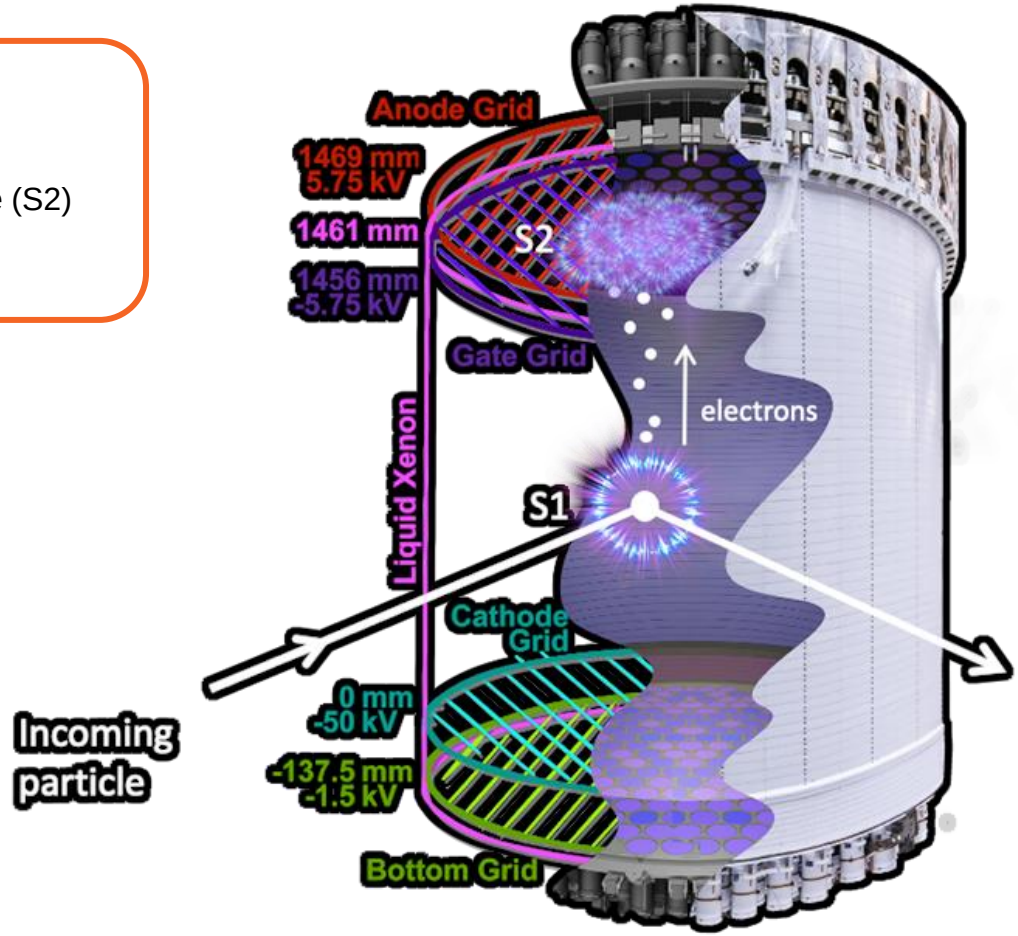

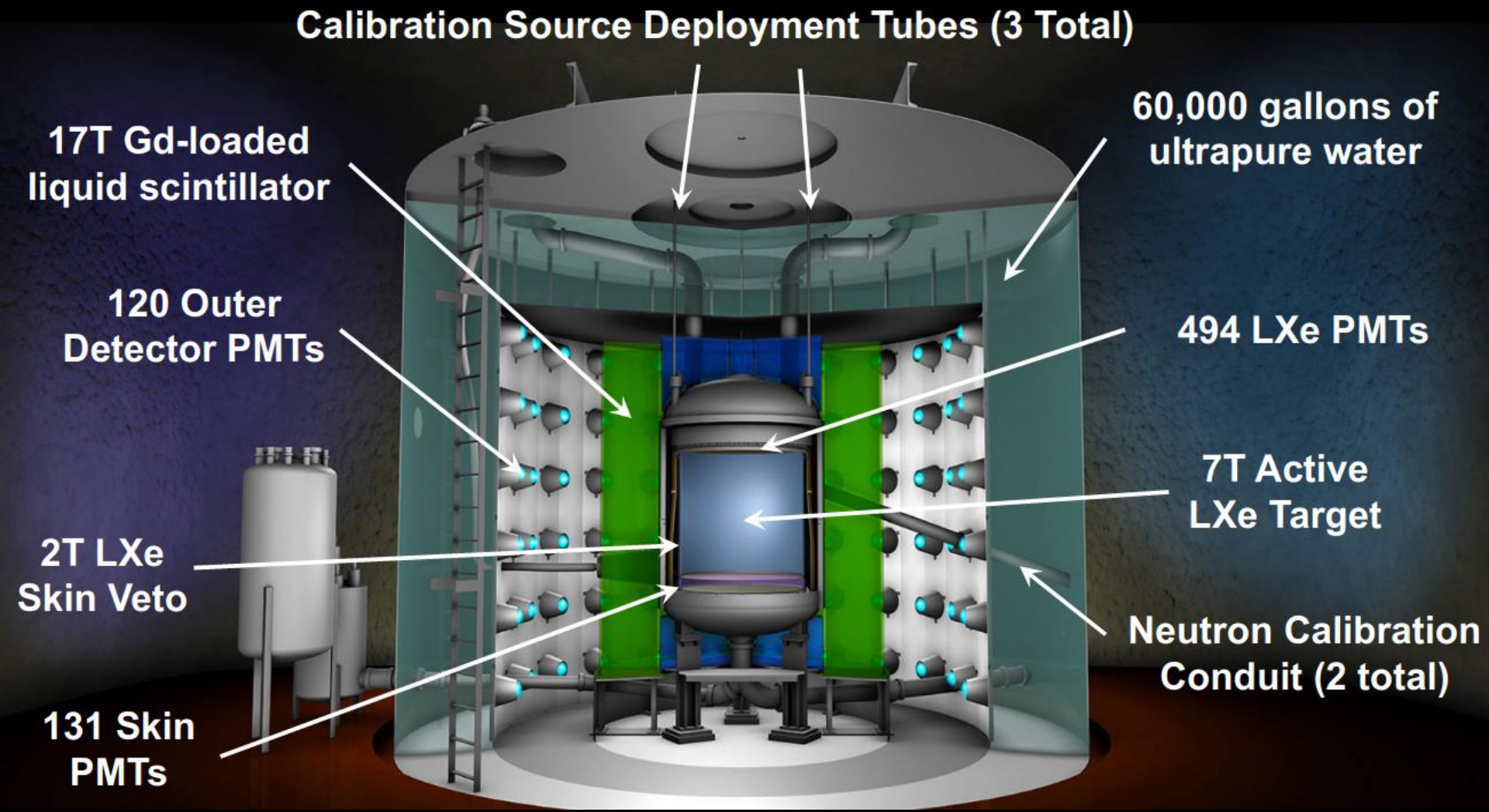
Calibration Source Deployment Tubes (3 Total)
17T Gd-loaded liquid scintillator
60,000 gallons of ultrapure water
120 Outer Detector PMTs
494 LXe PMTs
7T Active LXe Target
2T LXe Skin Veto
Neutron Calibration Conduit (2 total)
131 Skin PMTs

SR1 Overview

Detector Conditions
- **Drift field: 193 V/cm**
- Extraction field: 7.3 kV/cm in gas
- >97% if PMTs operational
- Liquid temperature (174.1 K)
- 3.3 t/day Xe purified through hot getter

Dataset
- Data taken Dec.2022-May.2023
- **60±1 live days**
- **5.5±0.2 tonne fiducial volume**
- Photon collection efficiency: g1=0.114±0.2 phd/photon
- Charge gain: g2=47.1±1.1 phd/electron

Analysis
- ER Calibrations (Tritium)
- NR Calibrations (Deuterium-Deuterium)
- Backgrounds well modelled in energy region (see Phys. Rev. D 108, 012010)
- Unbinned profile likelihood in $\log_{10}(S2_c)-S1_c$
- Paper: Phys. Rev. Lett. 131, 041002

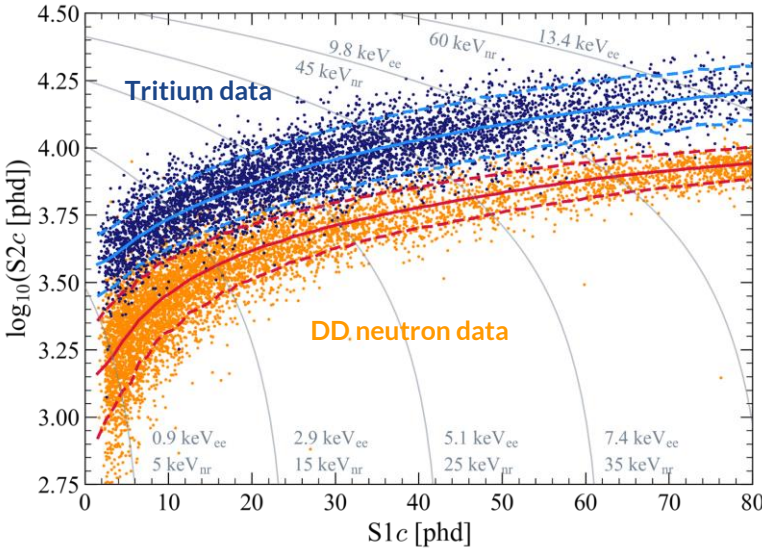

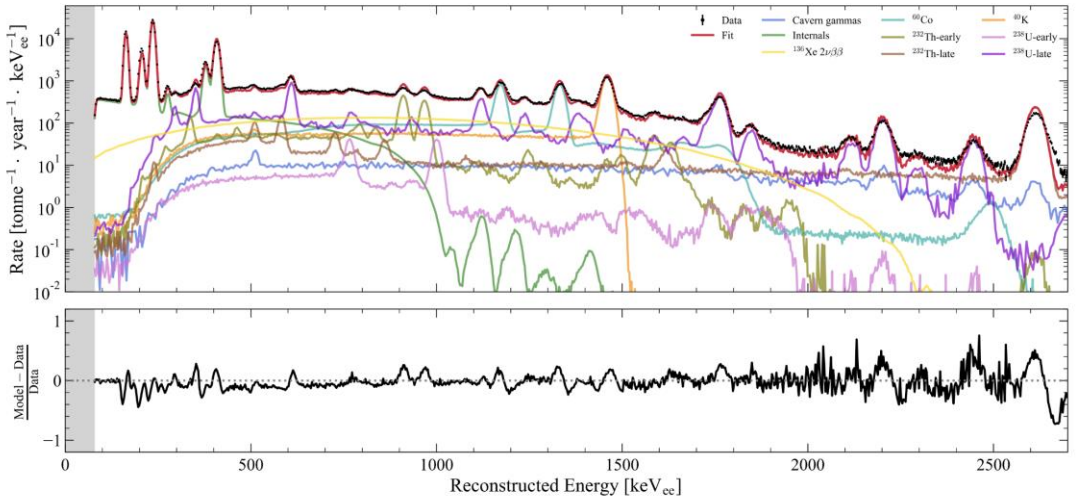

SR1 Dark Matter Search Results

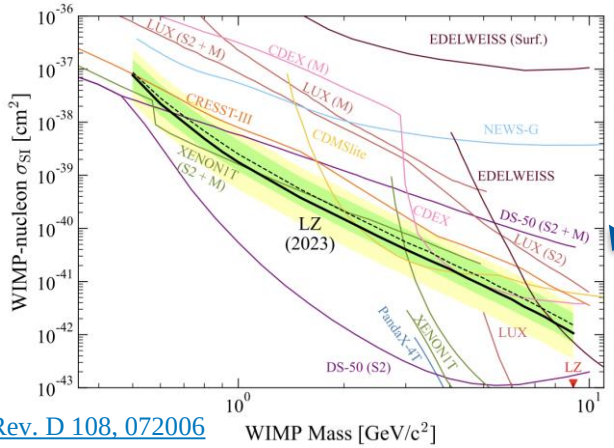

Phys. Rev. D 108, 072006

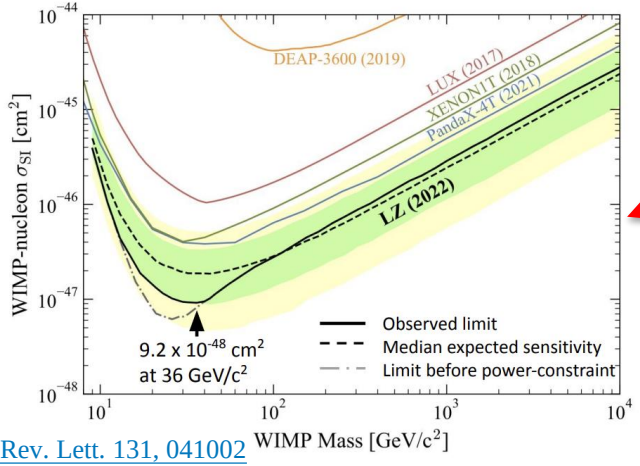

Phys. Rev. Lett. 131, 041002

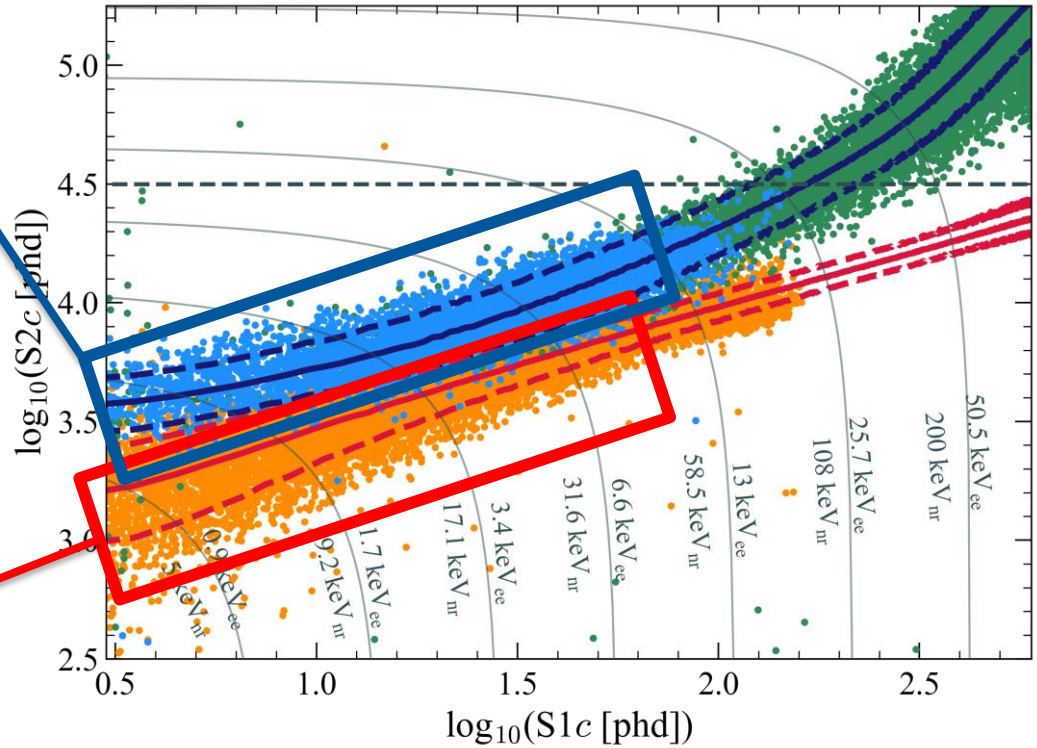

Non-Relativistic Effective Field Theory: Operators

Phys. Rev. C 89, 065501 (2014)
JCAPO2 (2013)

- Spin Independent and Spin Dependent interactions rely on the assumption of a zero-momentum transfer. But what if there is some momentum dependency?

- Use an EFT where we treat the WIMP-nucleon elastic scattering as a four-field interaction

$$\mathcal{L}_{int} = \mathcal{O}\chi^{+}\chi^{-}N^{+}\mathrm{N}^{-}$$

- 4 Galilean, Hermitian invariants quantities which describe the interaction

$$i\vec{q}, \vec{S}_{\chi}, \vec{S}_{N}, \vec{v}^{\perp} \equiv \vec{v} + \frac{\vec{q}}{2\mu_N}$$

- We are then left with 15 operators which contribute to the interaction Lagrangian

$$\mathcal{L}_{int} = \sum_{i} c_i \mathcal{O}_i$$
$$= c_1 + ic_3\vec{S}_N \cdot (\vec{q} \times \vec{v}^{\perp}) + c_4\vec{S}_{\chi} \cdot \vec{S}_N + ic_5\vec{S}_{\chi} \cdot (\vec{q} \times \vec{v}^{\perp}) + c_6(\vec{S}_{\chi} \cdot \vec{q})(\vec{S}_N \cdot \vec{q}) + c_7\vec{S}_N \cdot \vec{v}^{\perp} + c_8\vec{S}_{\chi} \cdot \vec{v}^{\perp} + ic_9\vec{S}_{\chi} \cdot (\vec{S}_N \times \vec{q}) + c_{10}\vec{S}_N \cdot \vec{q} + ic_{11}\vec{S}_{\chi} \cdot \vec{q} + c_{12}\vec{S}_{\chi} \cdot (\vec{S}_N \times \vec{v}^{\perp}) + ic_{13}(\vec{S}_{\chi} \cdot \vec{v}^{\perp})(\vec{S}_N \cdot \vec{q}) + ic_{14}(\vec{S}_{\chi} \cdot \vec{q})(\vec{S}_N \cdot \vec{v}^{\perp}) + -c_{15}(\vec{S}_{\chi} \cdot \vec{q})\left((\vec{S}_N \times \vec{v}^{\perp}) \cdot \vec{q}\right)$$

- Differential Recoil Rate in this case

$$\frac{dR}{dE_R} = \frac{\rho_{\chi}}{32\,\pi m_{\chi}^3 m_N^2} \int_{v>v_{min}}^{\infty} \frac{f(\vec{v})}{v} \sum_{i,j=1}^{15} \sum_{a,b=0,1} c_j^a c_i^b F_{i,j}^{a,b} d^3v$$

- This framework can also be mapped onto covariant Lagrangians, allowing for more complex interactions to be studied (coming in a future paper).

NREFT Operator Signals

Evaluate the scattering amplitude assuming a single operator

$$\frac{dR}{dE_R} \rightarrow \frac{\rho_\chi c_i^2}{32\,\pi m_\chi^3 m_N^2} \int_{v>v_{min}}^{\infty} \frac{f(\vec{v})}{v} F_{i,i} d^3v$$

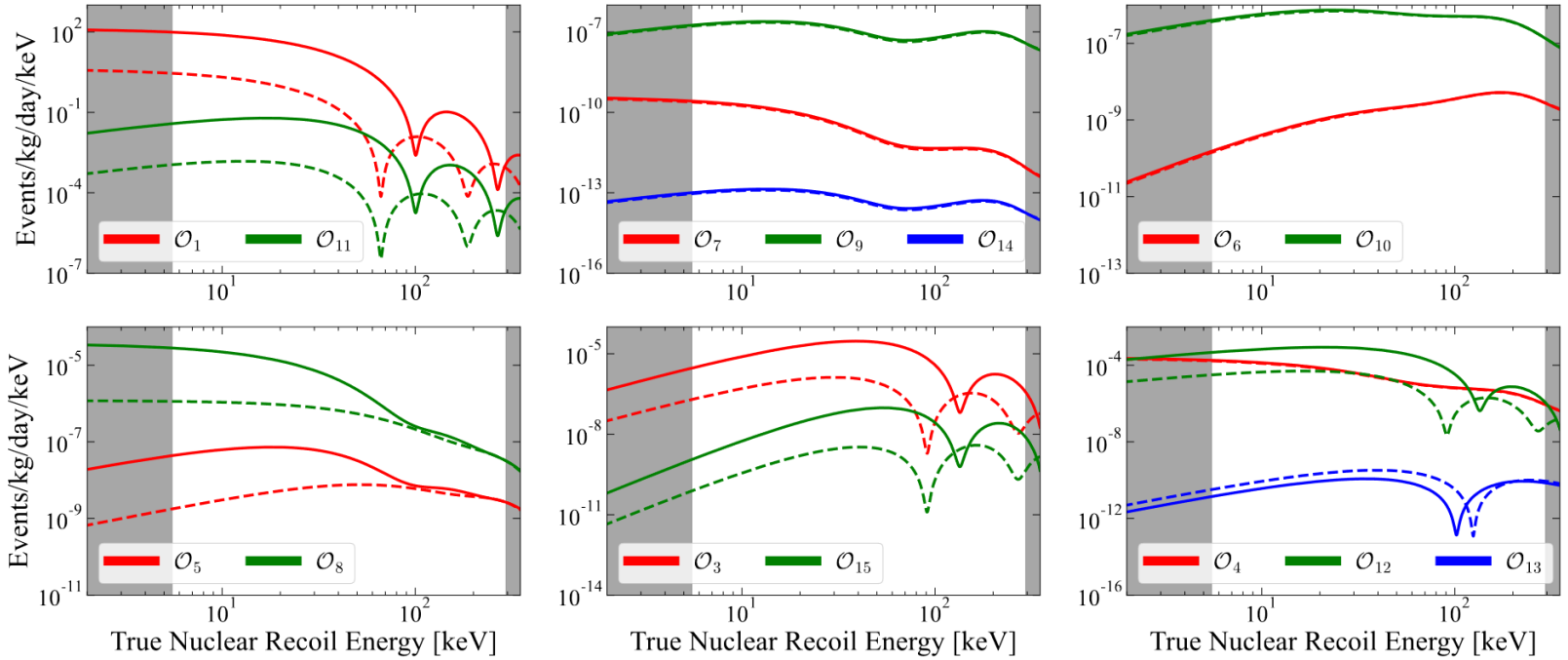

m_χ=1000 GeV/c^2
Solid lines: isoscalar
Dashed lines: isovector

Shaded region:
Energy where the efficiency for the LZ SR1 WIMP-Search data is <50%
After all cuts and ROI selection

Backgrounds in an extended energy analysis

All backgrounds relevant to SI WIMP search
Additional backgrounds

- Additional Xe decays
  - (^{124}Xe, ^{133}Xe, ^{131m}Xe, ^{127}Xe)
- Additional ER
- Topologies of more complex interactions (eg multiple scatter signal ionization events)

Source	Expected Events
Flat ER	517.4 ± 82.8
Detector ER	18.4 ± 9.2
ν ER	55.3 ± 5.5
^{124}Xe	8.2 ± 2.0
^{127}Xe	20.5 ± 1.8
^{136}Xe	55.1 ± 11.6
^{125}I	30.1 ± 15.6
^{8}B CEνNS	0.14 ± 0.01
Accidentals	1.3 ± 0.3
Subtotal	706 ± 86
^{37}Ar	[0, 288]
Detector neutrons	$0.0^{+0.5}$

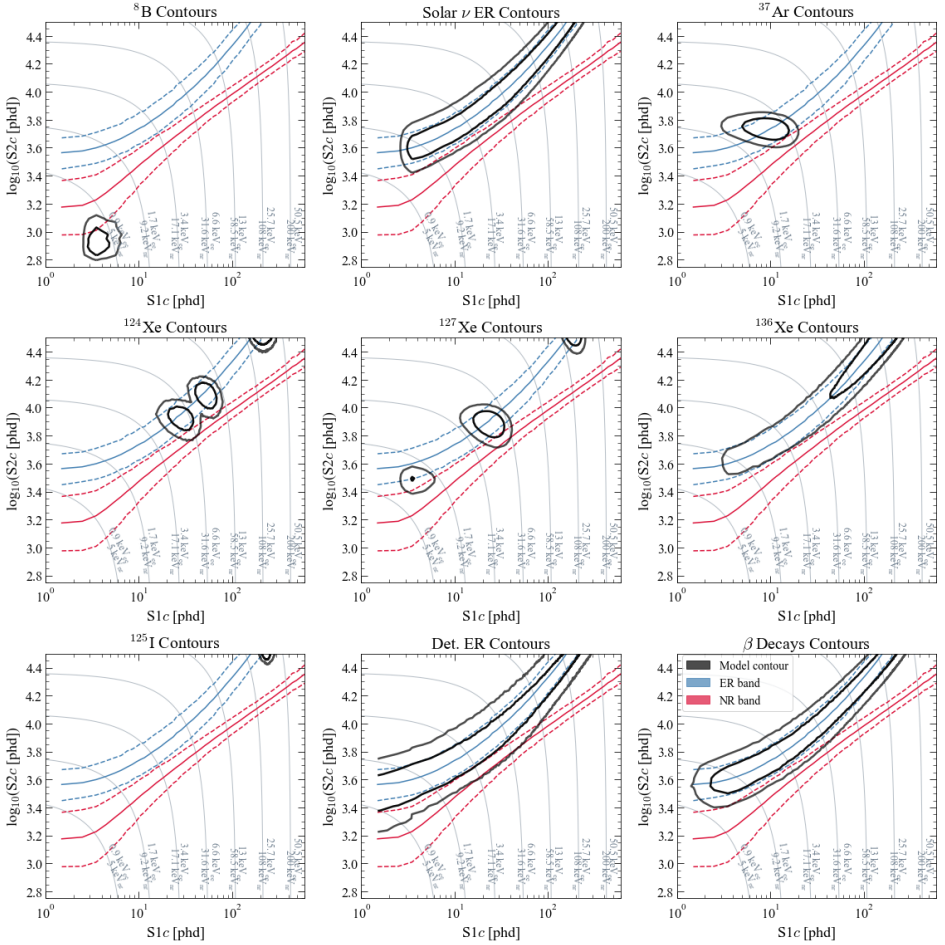

Multiple Scatter Single Ionisation Events

A γ-X event is a multiple-scattering γ where at least one vertex is in a region of incomplete charge collection:

- Reverse field region
- Near the TPC walls

Sources include:

- ^{238}U, ^{232}Th, ^{60}Co, ^{40}K from cathode
- ^{127}Xe near detector edges

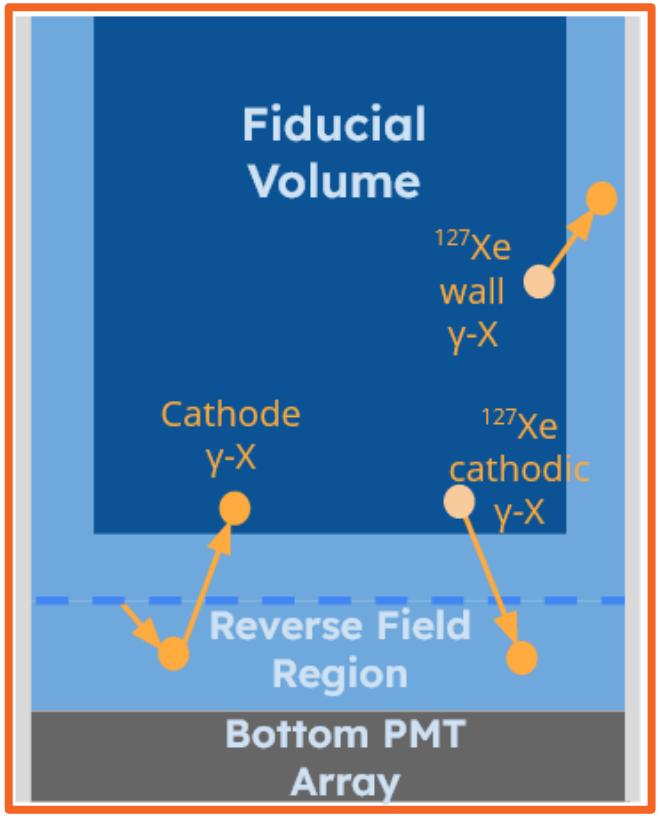

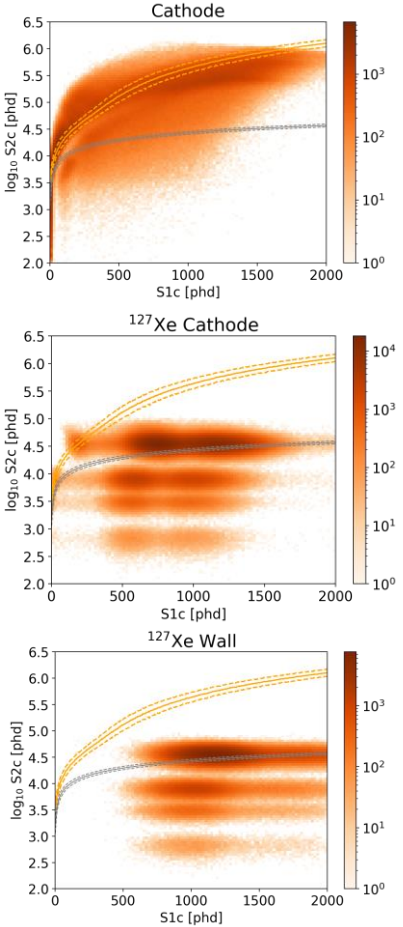

Multiple Scatter Single Ionisation Events - Classifying

Boosted Decision Tree cut trained on high stats simulations and calibration data

↓ P, → T	SS	γ-X
SS	99.997 ± 0.005	0.4 ± 1.2
γ-X	0.003 ± 0.005	99.6 ± 1.2

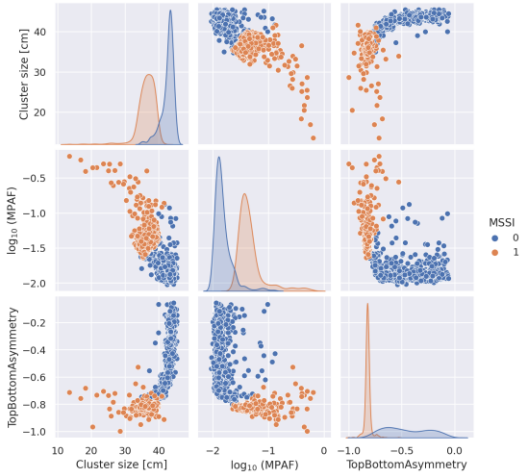

Quantities used in the classification:

- Cluster size (size of the S1 splash on the bottom PMT array)
- Max Peak Area Fraction
- Top Bottom Asymmetry
- S1c
- $\log_{10}$ S2c
- Radius
- Drift Time

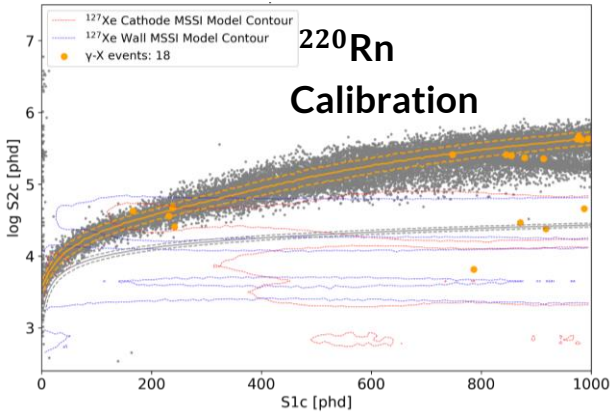

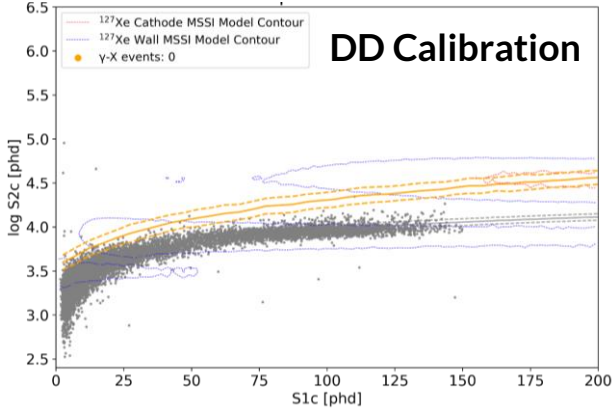

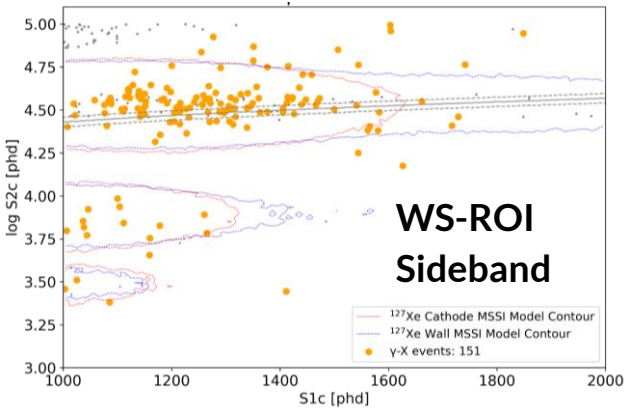

Dataset

Region of Interest

- 3 < S1c < 600 photons detected
- Three-fold PMT coincidence
- S2 > 600 phd
- Log10(S2c) < 4.5

Fiducial Volume

- Radial cut for <0.01 wall BGs
- 86 us < drift < 936.5 us
- 5.5±0.2 tonnes

Key

- Events surviving all selections
- OD tagged events
- Skin tagged events
- MSSI tagged events

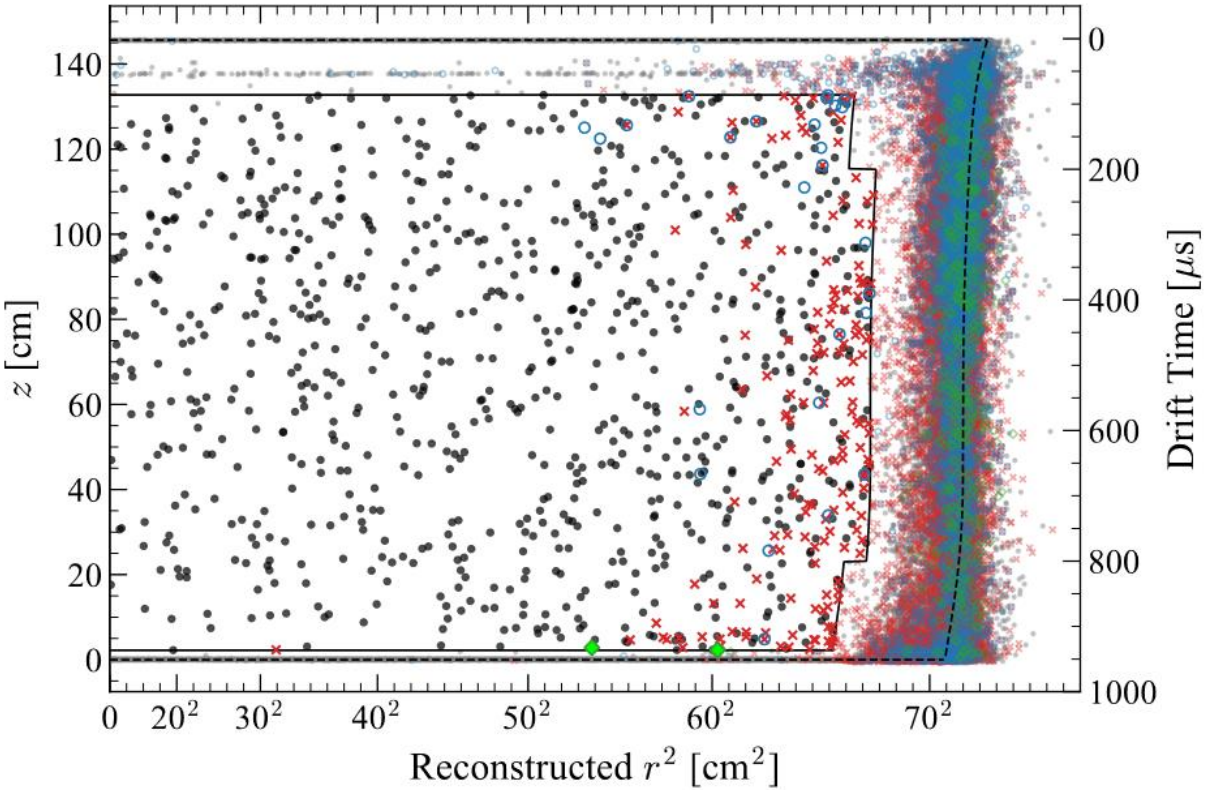

Data and Models

- 835 events
- PDFs created via energy deposit and detector response simulations

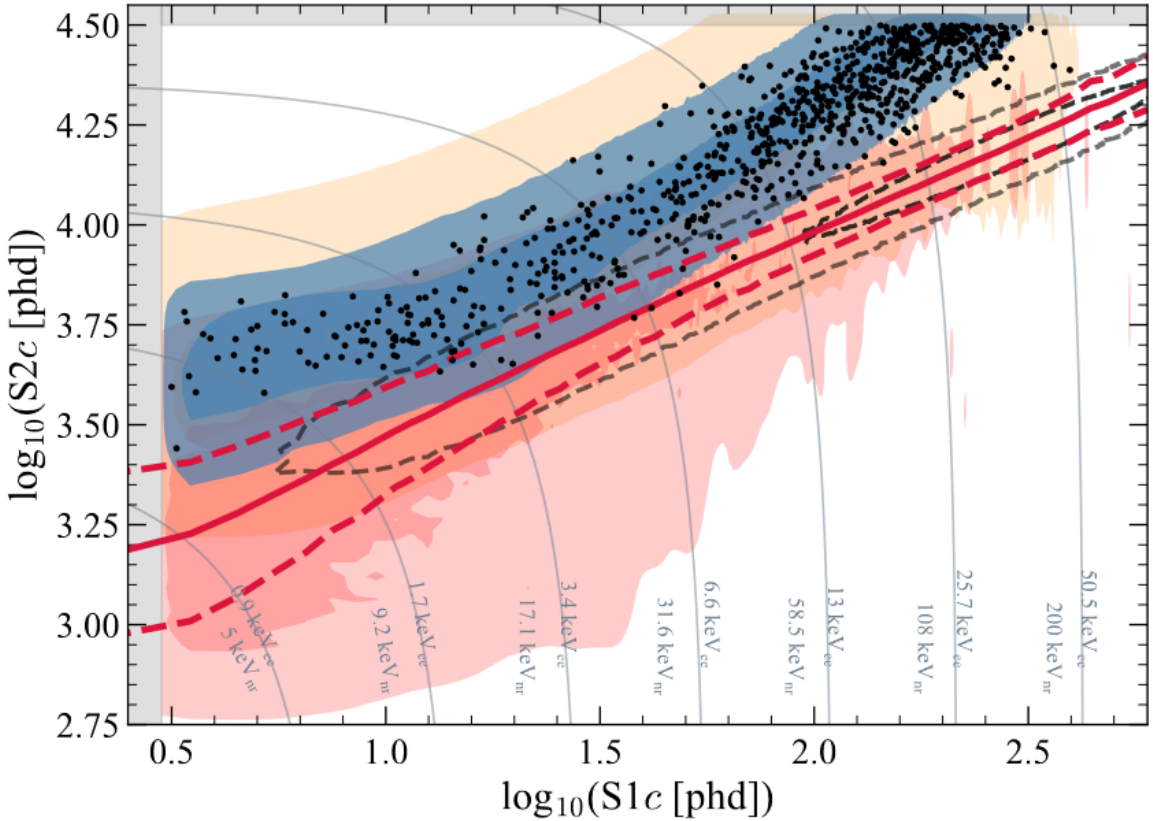

Model Key

- 1000 GeV/c² $\mathcal{O}_6^S$ WIMP
- Detector NR
- Detector ER
- Combined ER
- NR band from DD

Results from SR1

With this extended ROI we can test a large range of models.

Search performed;

- $\mathcal{O}_1 - \mathcal{O}_{15}$
- isoscalar and isovector basis
- elastic and inelastic

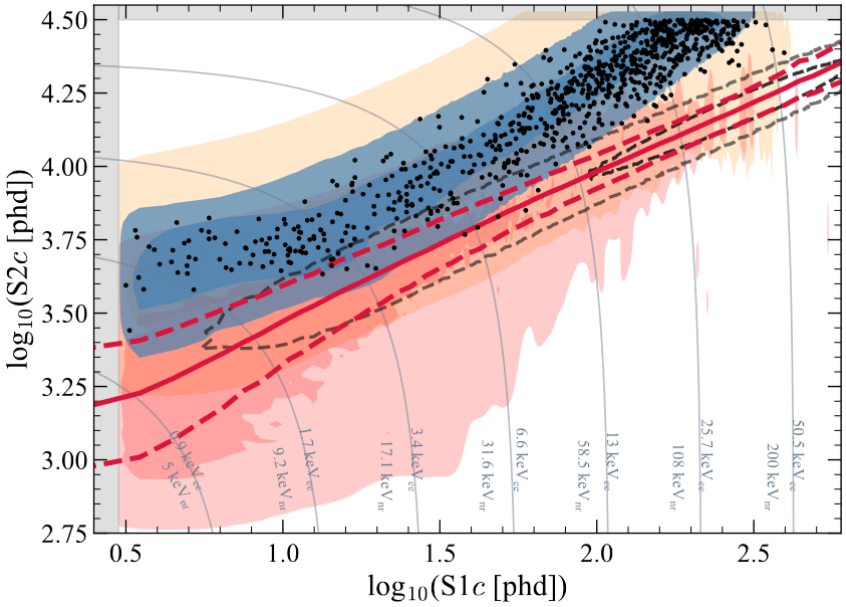

Source	Expected Events	Fit Result
Flat ER	517.4 ± 82.8	574.7 ± 30.2
Detector ER	18.4 ± 9.2	22.3 ± 8.1
ν ER	55.3 ± 5.5	55.5 ± 5.5
^{124}Xe	8.2 ± 2.0	8.7 ± 2.0
^{127}Xe	20.5 ± 1.8	20.8 ± 1.8
^{136}Xe	55.1 ± 11.6	58.2 ± 11.2
^{125}I	30.1 ± 15.6	34.2 ± 8.9
^{8}B CEνNS	0.14 ± 0.01	0.14 ± 0.01
Accidentals	1.3 ± 0.3	1.3 ± 0.03
Subtotal	706 ± 86	775 ± 34
^{37}Ar	[0, 288]	49.5 ± 9.4
Detector neutrons	$0.0^{+0.5}$	$0.0^{+1.8}$
Total	-	825 ± 36

arXiv:2312.02030

Results from SR1

With this extended ROI we can test a large range of models.

Search performed;

- $\mathcal{O}_1 - \mathcal{O}_{15}$
- isoscalar and isovector basis
- elastic and inelastic

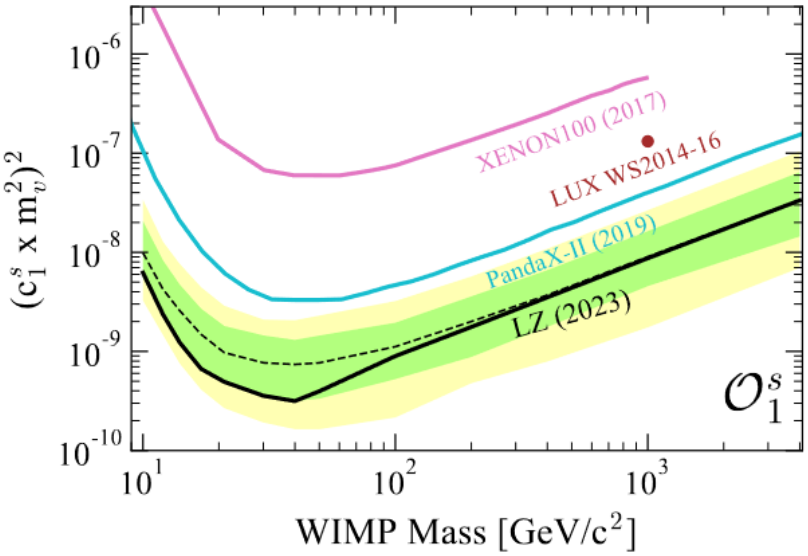

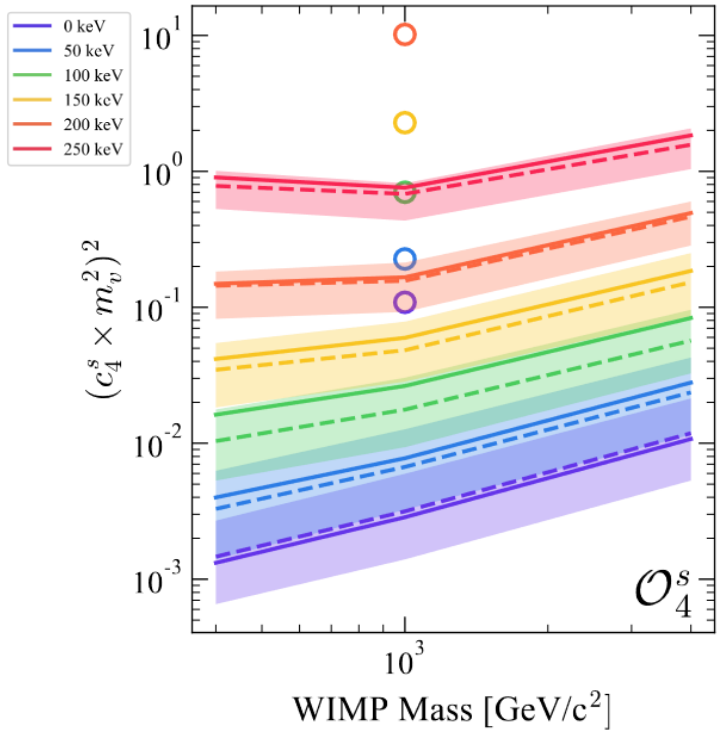

arXiv:2312.02030

LZ EFT Operator Results

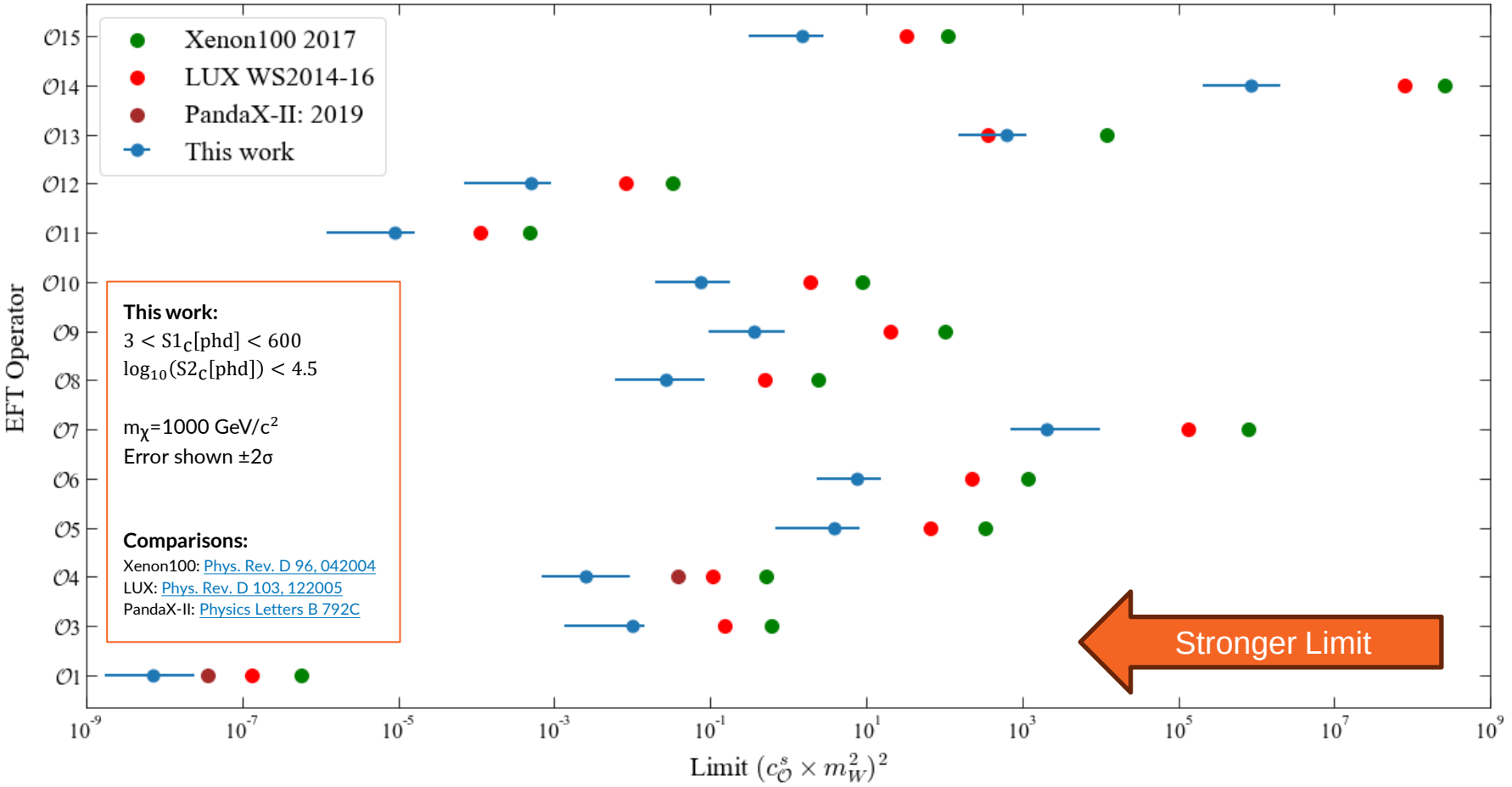

Summary

- Initial science run of LZ has placed stringent limits on both SI and SD WIMP-nucleon interactions
- These models are relatively simplistic, and the inherent nature of interaction may be more complex
- Using an EFT allows us to describe all possible dark matter interactions with nucleons
- Extending energy region is beneficial for EFT analysis
- LZ has set promising EFT limits in SR1 with an extended energy ROI so we are ready for more data
- With the energy region understood in LZ, we can test a lot of DM parameter space, eg:
  - 2HDM+a: Phys. D. M. 27, 100351 (2020)
  - DM –photon interactions: Nature **618**, 47 (2023)

LZ Publications:

- Detector paper: Nucl. Instrum. Meth. A 953, 163047
- SR1 papers:
  - WIMP-nucleon result: Phys. Rev. Lett. 131, 041002
  - Backgrounds: Phys. Rev. D 108, 012010
  - LowE ER: Phys. Rev. D 108, 072006
  - this work: Operators arXiv:2312.02030
    Lagrangians (paper in progress)

University of BRISTOL

Questions?

Science and Technology Facilities Council

Sanford Underground Research Facility
South Dakota Science and Technology Authority

FCT
Fundação para a Ciência e a Tecnologia
MINISTÉRIO DA EDUCAÇÃO E CIÊNCIA

ibs Institute for Basic Science

Efficiency of data selection

Cut Development
- Non-WIMP ROI
- Calibration data

Event Selection
- Single Scatter
- Fiducial Volume
- Region-of-Interest
- S1/S2 shape cuts
- Veto detector anti-coincidence

Rejection of livetime
- When detector was unstable
- High TPC rates

60.3±1.2 live days

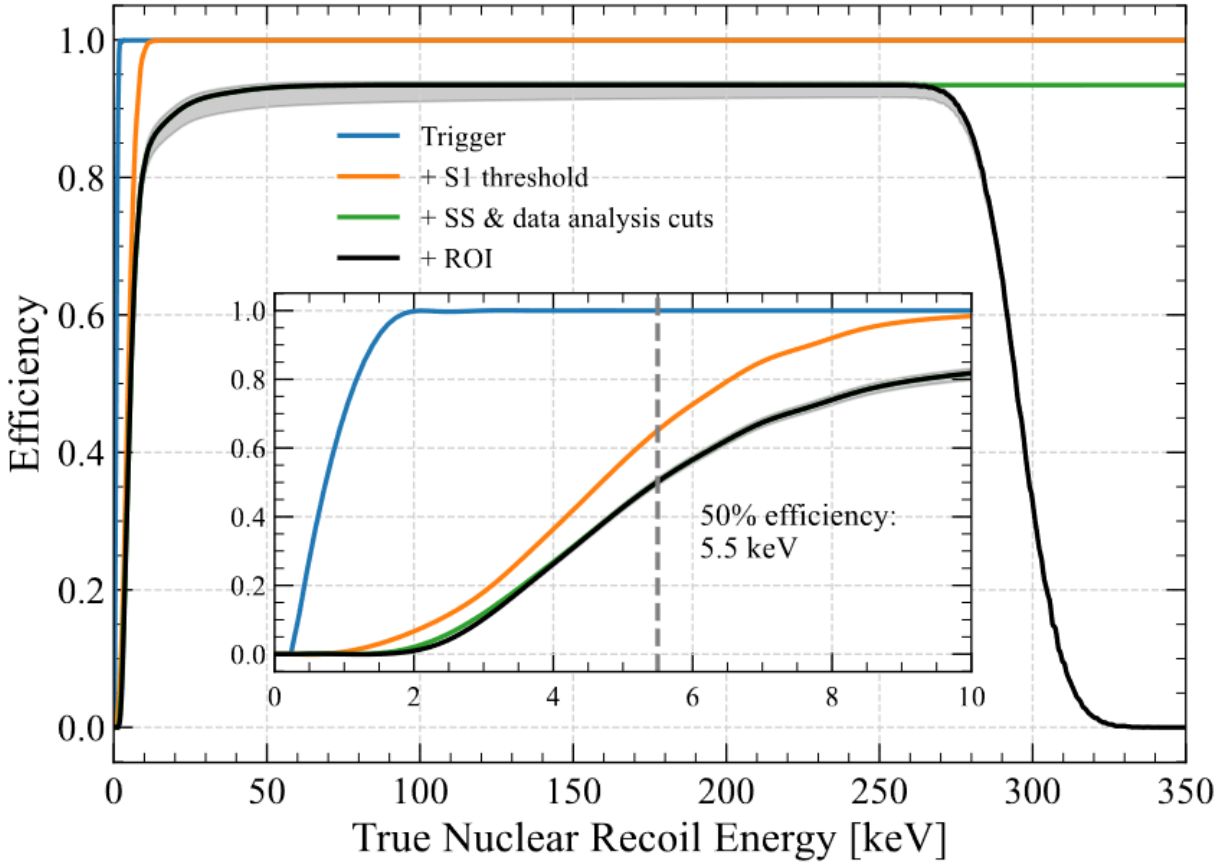

Machine Learning Boosted Decision Tree for γ-X

Boosted Decision Tree cut trained on high stats simulations and calibration data

↓ P, → T	SS	γ-X
SS	99.997 ± 0.005	0.4 ± 1.2
γ-X	0.003 ± 0.005	99.6 ± 1.2

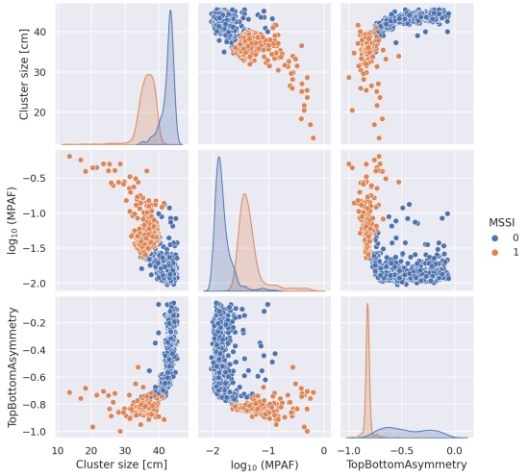

Quantities used in the classification:

- Cluster size (size of the S1 splash on the bottom PMT array)
- Max Peak Area Fraction
- Top Bottom Asymmetry
- S1c
- $\log_{10}$ S2c
- Radius
- Drift Time

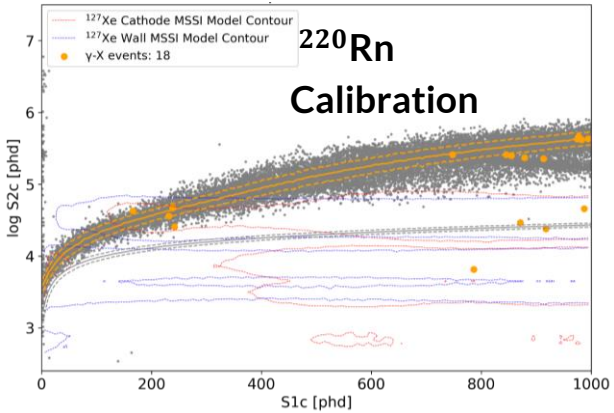

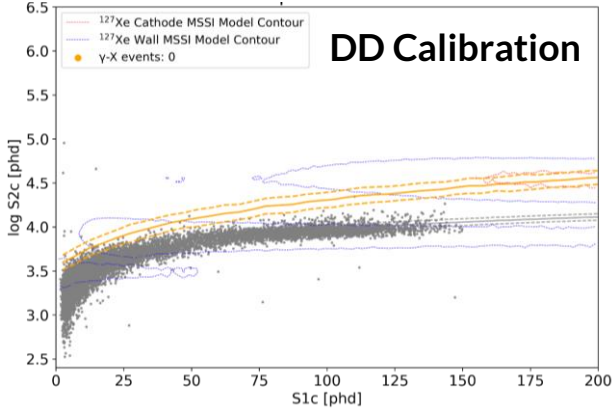

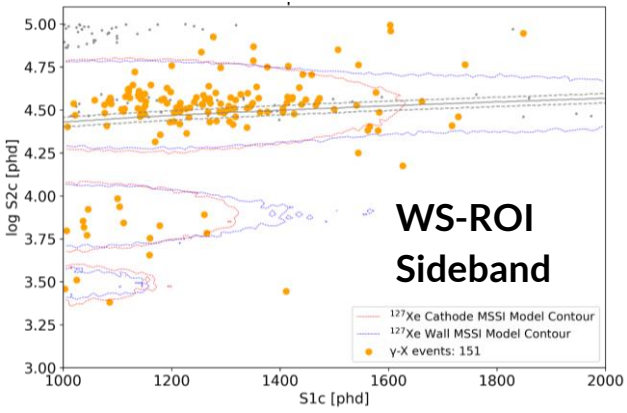

Non-Relativistic Effective Field Theory: Operators

Galilean-invariant to quadratic order in momentum transfer

Spin 1 or less particles

$$i\vec{q},\ \vec{S}_\chi,\ \vec{S}_N,\ \vec{v}^{\perp} \equiv \vec{v} + \frac{\vec{q}}{2\mu_N}$$

Theory translated to coefficients of an effective operator

These operators can be equated to generic nuclear responses

Possible to reduce covariant interaction Lagrangians to combinations of the operators

$$\begin{aligned}\mathcal{L}_{int} &= \sum_i c_i \mathcal{O}_i \\ &= c_1 + ic_3\vec{S}_N \cdot (\vec{q} \times \vec{v}^{\perp}) + c_4\vec{S}_\chi \cdot \vec{S}_N \\ &+ ic_5\vec{S}_\chi \cdot (\vec{q} \times \vec{v}^{\perp}) + c_6(\vec{S}_\chi \cdot \vec{q})(\vec{S}_N \cdot \vec{q}) \\ &+ c_7\vec{S}_N \cdot \vec{v}^{\perp} + c_8\vec{S}_\chi \cdot \vec{v}^{\perp} + ic_9\vec{S}_\chi \cdot (\vec{S}_N \times \vec{q}) \\ &+ c_{10}\vec{S}_N \cdot \vec{q} + ic_{11}\vec{S}_\chi \cdot \vec{q} + c_{12}\vec{S}_\chi \cdot (\vec{S}_N \times \vec{v}^{\perp}) \\ &+ ic_{13}(\vec{S}_\chi \cdot \vec{v}^{\perp})(\vec{S}_N \cdot \vec{q}) + ic_{14}(\vec{S}_\chi \cdot \vec{q})(\vec{S}_N \cdot \vec{v}^{\perp}) \\ &+ -c_{15}(\vec{S}_\chi \cdot \vec{q})\left((\vec{S}_N \times \vec{v}^{\perp}) \cdot \vec{q}\right)\end{aligned}$$

Interactions are linear combinations of 6 independent nuclear responses

- M Spin Independent
- Σ' Spin Dependent (transverse)
- Σ'' Spin Dependent (longitudinal)
- Δ Angular Momentum
- Φ'' Spin Orbit
- $\tilde{\phi}'$ Tensor spin orbit

$$\frac{dR}{dE_R} = \frac{\rho_\chi}{32\,\pi m_\chi^3 m_N^2} \int_{v>v_{min}}^{\infty} \frac{f(\vec{v})}{v} \sum_{i,j=1}^{15} \sum_{a,b=0,1} c_j^a c_i^b F_{i,j}^{a,b} d^3v$$

Operators give us a sense of the true sensitivity of our detector to different DM-nucleon physics

Phys. Rev. C 89, 065501 (2014)

Benefit from an increased energy window

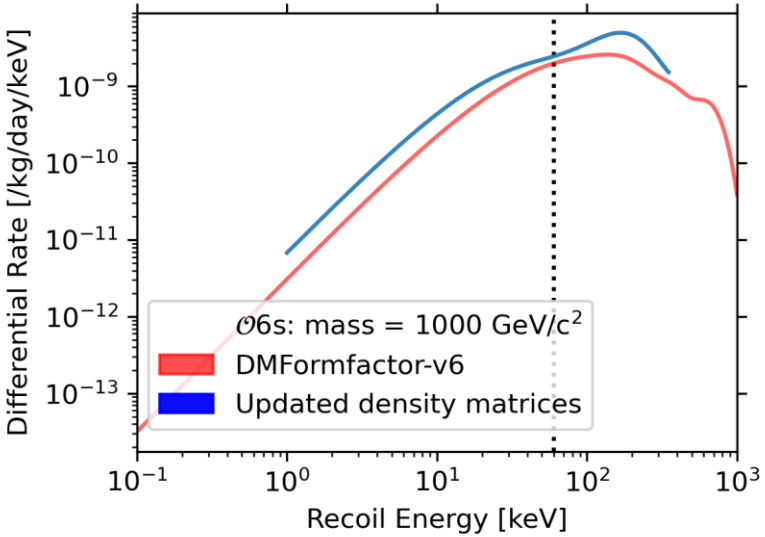

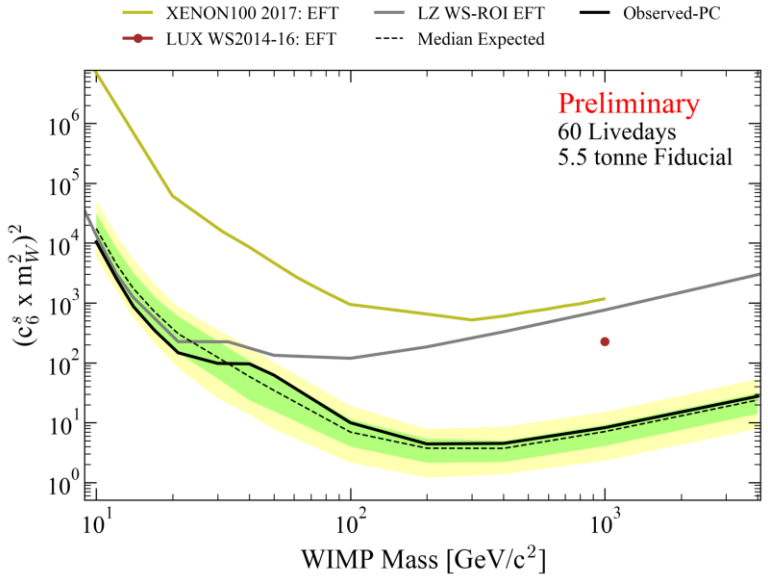

Dashed line indicates the energy at falling edge of the efficiency is 50% with LZ SR1 WIMP-Search ROI:

- $3 < S1_c[\text{phd}] < 80$

Grey:

- $3 < S1_c[\text{phd}] < 80$
- DMFormFactor-v6 signal

Black + Brazilian band (this work):

- $3 < S1_c[\text{phd}] < 600, \log_{10}(S2_c[\text{phd}]) < 4.5$
- Updated density matrices for signals

LZ EFT Preliminary Results

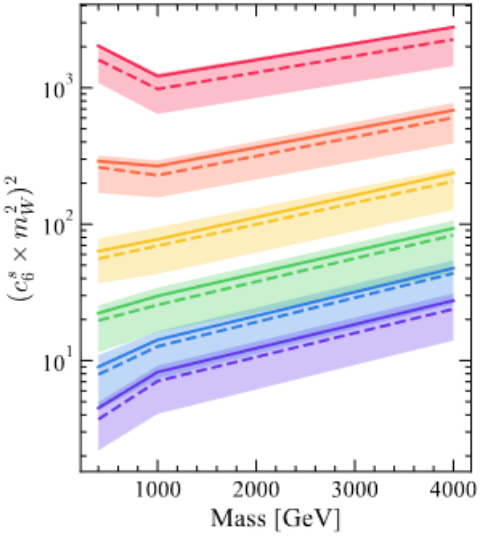

Inelastic Operators

This work:

- $3 < \mathrm{S1_C[phd]} < 600$
- Updated density matrices for signals

$$\delta_m \equiv m_{\chi,out} - m_{\chi,in}$$

$$\delta_m + \vec{v} \cdot \vec{q} + \frac{|\vec{q}|^2}{2\mu_N} = 0$$

$$\vec{v}_{inel}^{\perp} \equiv \vec{v} + \frac{\vec{q}}{2\mu_N} + \frac{\delta_m}{|\vec{q}|^2}\vec{q}$$

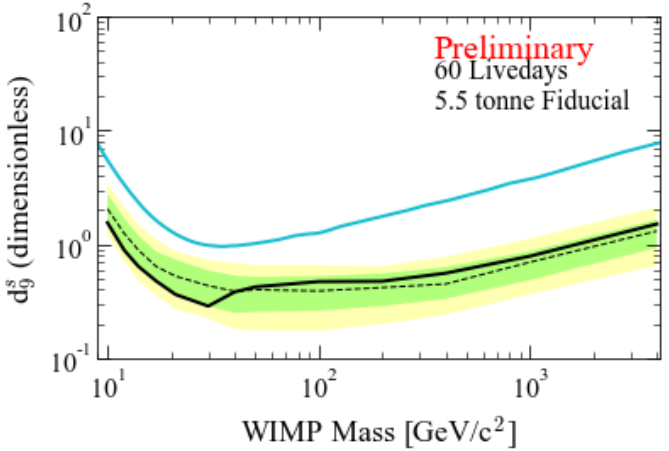

Elastic Lagrangians

This work:

- $3 < \mathrm{S1_C[phd]} < 600$
- Updated density matrices for signals

Blue:

- PandaX-II: Physics Letters B 792C

$$\mathcal{L}_{int}^{9} \rightarrow -\frac{\vec{q}^2}{2m_\chi m_M}\mathcal{O}_1 + \frac{2m_N}{m_M}\mathcal{O}_5 - \frac{2m_N}{m_M}\left(\frac{\vec{q}^2}{m_M}\mathcal{O}_4 - \mathcal{O}_6\right)$$

$$\mathcal{L}_{int}^{17} \rightarrow \frac{2m_N}{m_M}\mathcal{O}_{11}$$

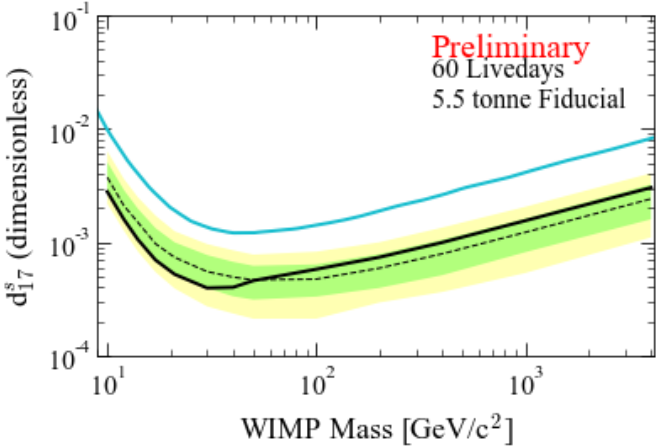

Impacts from updated nuclear density matrices

Differential recoils used updated GCN5082 ground state to ground state one-body density matrices

These have significant impacts on some operators

$\mathcal{O}_{13}$ differential rate has decreased significantly

$\mathcal{O}_{14}$ has the opposite behaviour

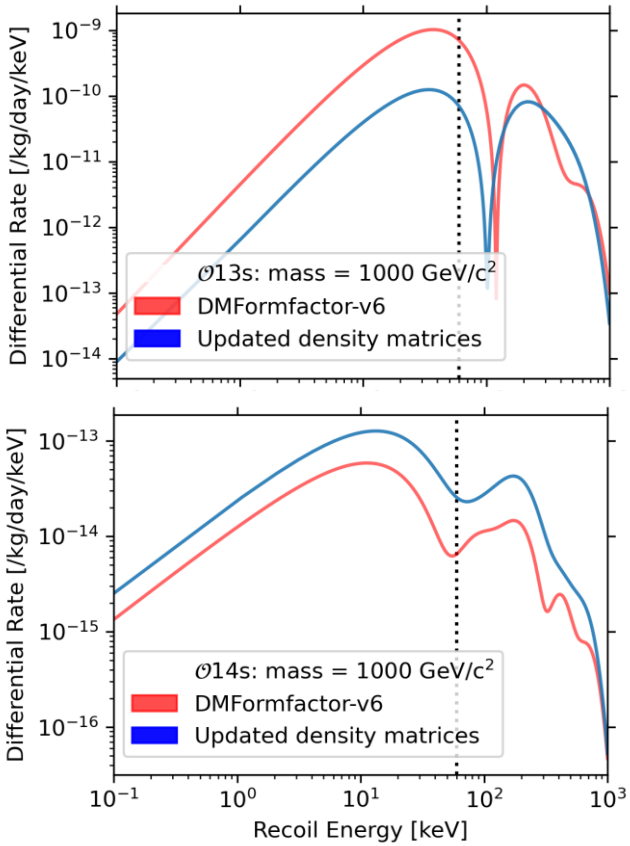

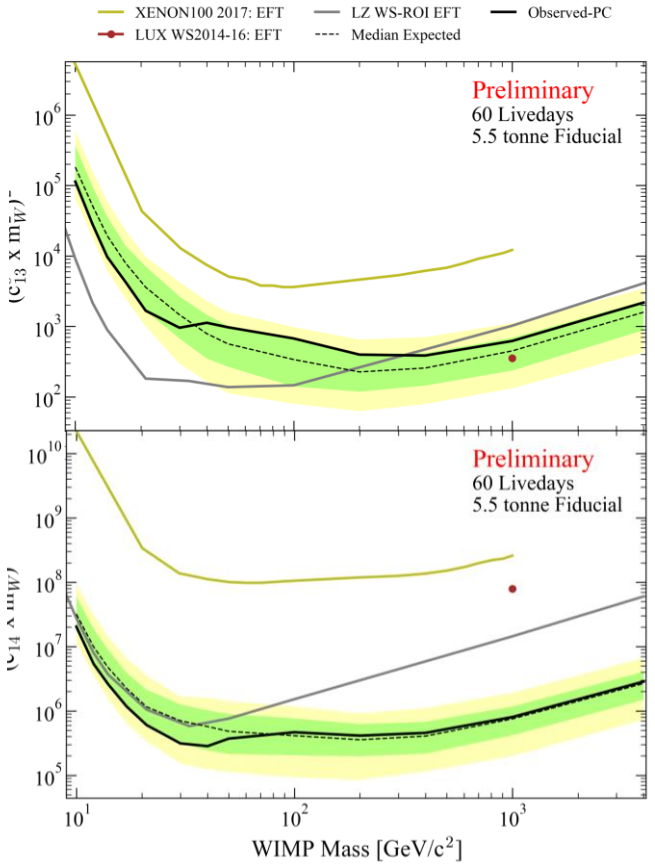

The LUX-ZEPLIN Detector

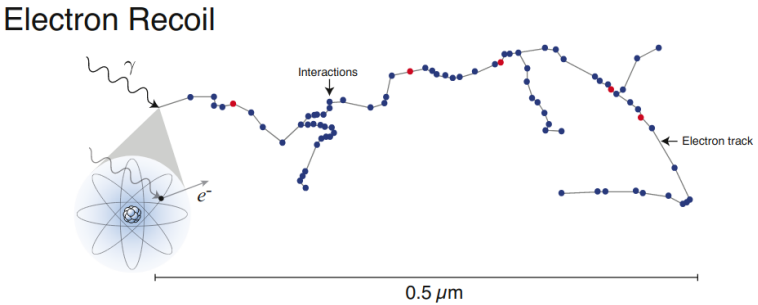

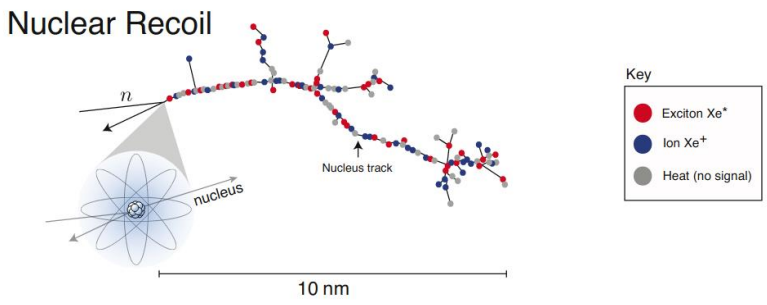

Dual Phase Time Projection Chamber

- Primary scintillation light (S1)
- Secondary scintillation induced from free charge (S2)
- 3D reconstruction allows for fiducialisation
- ER/NR discrimination from S1:S2 ratio